Electronic Supplementary Information

Changing the Bridging Connectivity Pattern within Heterometallic Assembly: Design of Single-Source Precursors with Discrete Molecular Structure

Zheng Wei, Haixiang Han, Alexander S. Filatov, Evgeny V. Dikarev*

Department of Chemistry, University at Albany, Albany, NY 12222, USA.

*Author to whom correspondence should be addressed. E-mail: edikarev@albany.edu. Phone: (518)442-4401. Fax: (518)442-3462.

Content

Experimental section. General procedures

All of the manipulations were carried out in a dry, oxygen-free argon atmosphere by employing standard Schlenk and glove box techniques. Anhydrous cobalt(II) chloride ($CoCl_2$), lithium methoxide (LiOMe), lithium acetylacetonate (Li(acac)), *tert*-butyl acetoacetate (Htbaoac), cobalt(II) chloride hexahydrate ($CoCl_2{\cdot}6H_2O$), triethylamine (NEt_3), and 2,2-dimethyl-hexanedione (Hdhd) were purchased from Sigma-Aldrich and used upon received. The attenuated total reflection (ATR) spectra were recorded on a PerkinElmer Spectrum 100FT-IR spectrometer. NMR spectra were obtained on a Bruker Avance 400 spectrometer at 400 MHz for ^{1}H and at 155.5 MHz for ^{7}Li. Chemical shifts (δ) are given in ppm relative to the residual solvent peaks for ^{1}H, and to the ^{7}Li peak of external standard (0.1 M solution of LiCl in d_8-THF). Thermal decomposition of heterometallic precursors was studied in air or oxygen atmosphere at ambient pressure. The solid sample (*ca.* 40 mg) was placed into a 20 mL Coors high-alumina crucible (Aldrich) and heated at a rate of *ca.* 35 °C/min in a muffle furnace (Lindberg Blue M). The decomposition residues were analyzed by X-ray powder diffraction. X-ray powder diffraction data were collected on a Bruker D8 Advance diffractometer (Cu Kα radiation, focusing Göbel Mirror, LynxEye one-dimensional detector, step of 0.02^o 2θ, 20 °C). The crystalline samples under investigation were ground and placed in the dome-like airtight zero-background holders inside a glove box. Le Bail fit for powder diffraction patterns has been performed using TOPAS, version 4 software package (Bruker AXS, 2006). Elemental analysis has been performed by Complete Analysis Laboratories, Inc., Parsippany, NJ.

Synthesis of starting reagents

Li(tbaoac). A flask was charged with LiOMe (0.686 g, 18.07 mmol) under argon atmosphere, and 40 mL of dry, oxygen-free methanol were added. Upon stirring, Htbaoac (2.957 g, 3.1 mL) was added to the solution. The colorless solution was stirred at room temperature for 1 h. The solvent was evaporated under vacuum at room temperature. The white-colored final product was obtained by further drying the residue under vacuum at 80 °C overnight. Yield is *ca.* 2.818 g (95%). ^{1}H NMR (400 MHz, $CDCl_3$, 22 °C): δ 1.40 (s, $OC(CH_3)_3$); 1.94 (s, CH_3); 4.78 (s, CH). ^{7}Li NMR (155.5 MHz, THF, 22 °C): δ 1.26 (s). Compound is soluble in all common solvents, except hexanes. It can be recrystallized by cooling down its saturated solution in dichloromethane at -10 °C overnight. It starts to decompose at 180 °C in evacuated ampule, before any sublimation is visually observed.

Co(tbaoac)$_2$. The synthetic procedure was modified from that previously reported in the literature.[1] $CoCl_2\cdot 6H_2O$ (0.701 g, 2.95 mmol) was dissolved in 10 mL of water. Upon stirring, Htbaoac (0.954 g, 1 mL) dissolved in 2.5 mL of methanol was added. Triethylamine (0.610 g, 0.8 mL) solution in 2.5 mL of methanol was added dropwise to the reaction mixture. The solution was stirred for 0.5 h, and pink precipitate was formed gradually. The solid was filtered off and washed with water and cold methanol several times. The final purple product was obtained by further drying the residue under vacuum at 100 °C overnight. Yield is *ca.* 1.024 g (93%). Compound is soluble in all common solvents, except hexanes. It can be quantitatively sublimed at 150 °C in a sealed ampule and it is decomposed at around 170 °C.

Li(dhd). A flask was charged with LiOMe (0.219 g, 5.77 mmol) under argon atmosphere, and 20 mL of dry, oxygen-free methanol were added. Upon stirring, Hdhd (0.912 g, 1.0 mL) was added to the solution. The colorless solution was stirred at room temperature for 0.5 h. The solvent was evaporated under vacuum at room temperature. The white-colored final product was obtained by further drying the residue under vacuum at 80 °C overnight. Yield is *ca.* 0.795 g (93%). ^{1}H NMR (400 MHz, THF, 22 °C): δ 1.05 (s, Bu^t); 2.64 (s, Me); 5.27 (s, CH). ^{7}Li NMR (155.5 MHz, THF, 22 °C): δ 1.30 (s). Compound is only soluble in coordinating solvents such as acetone, ethanol and THF. It starts to decompose at 180 °C in evacuated ampule, before any sublimation is visually observed.

Synthesis of heterometallic precursors 1–3

LiCo(acac)$_3$ (1)

Method I. A mixture of Li(acac) (38 mg, 0.358 mmol) and $CoCl_2$ (15 mg, 0.116 mmol) was sealed in an evacuated glass ampule and placed in an electric furnace having a temperature gradient along the length of the tube. The ampule was kept at 170 °C for 12 days to allow needle-shaped pink crystals to be deposited in the cold section of the container where the temperature was set approximately 5 °C lower. Yield is *ca.* 35 mg (83%).

Method II. A flask was loaded with Li(acac) (2.500 g, 23.57 mmol) and $CoCl_2$ (1.011 g, 7.79 mmol) under argon atmosphere, and 100 mL of dry ethanol was added. The pink suspension was formed upon stirring for 2 h. The pink solid was filtered off, washed with ethanol several times and dried under vacuum at 120 °C overnight. Yield is *ca.* 2.742 g (97%). The purity of the crystalline product was confirmed by X-ray powder diffraction analysis (Fig. S1). Compound **1** is only soluble in strongly coordinating solvents, such as methanol, H_2O, DMSO and THF. It can be quantitatively resublimed at 170 °C in evacuated ampule and it is decomposed at the temperatures higher than 180 °C.

LiCo(tbaoac)$_3$ (2)

Method I. A flask was loaded with Li(tbaoac) (0.220 g, 1.34 mmol) and Co(tbaoac)$_2$ (0.500 g, 1.34 mmol) under argon atmosphere, and 50 mL of dry, oxygen-free dichloromethane was added. The purple solution was stirred at room temperature for 0.5 h. The solvent was evaporated under vacuum at room temperature. Yield is *ca.* 0.648 g (90%).

Method II. A flask was charged with Li(tbaoac) (0.380 g, 2.31 mmol) and $CoCl_2$ (0.100 g, 0.77 mmol) under argon atmosphere, and 100 mL of dry, oxygen-free ethanol was added. The purple solution was stirred at room temperature for 1 h. The solvent was evaporated under vacuum at room temperature and the pink-colored solid residue was further dried under vacuum at 80 °C overnight. The final purple product was isolated by dichloromethane extraction followed by evaporation of the solvent at room temperature. Yield is *ca.* 0.397 g (96%). The purity of the crystalline product consisting of two polymorph modifications was confirmed by X-ray powder diffraction analysis (Fig. S2). Compound **2** is soluble in all common solvents, but it has a limited solubility in hexanes. It can be quantitatively resublimed at 160 °C in evacuated ampule and it is decomposed at the temperatures higher than 170 °C.

LiCo(dhd)$_3$ (3). A flask was charged with Li(dhd) (0.380 g, 0.70 mmol) and $CoCl_2$ (0.03 g, 0.23 mmol) under argon atmosphere, and 20 mL of dry, oxygen-free ethanol was added. The dark-purple solution was stirred at room temperature for 1 h. The solvent was evaporated under vacuum at room temperature and the purple-colored solid residue was further dried under vacuum at 80 °C overnight. The final violet product was isolated by dichloromethane extraction followed by evaporation of the solvent at room temperature. Yield is *ca.* 0.107 g (95%). The purity of the crystalline product consisting of two polymorph modifications was confirmed by X-ray powder diffraction analysis (Fig. S3). Compound **3** is soluble in all common solvents, except hexanes. It can be quantitatively resublimed at 150 °C in evacuated ampule and it is decomposed at the temperatures higher than 170 °C.

X-ray powder diffraction patterns of $LiCoL_3$ (L = acac(1), tbaoac(2) and dhd(3))

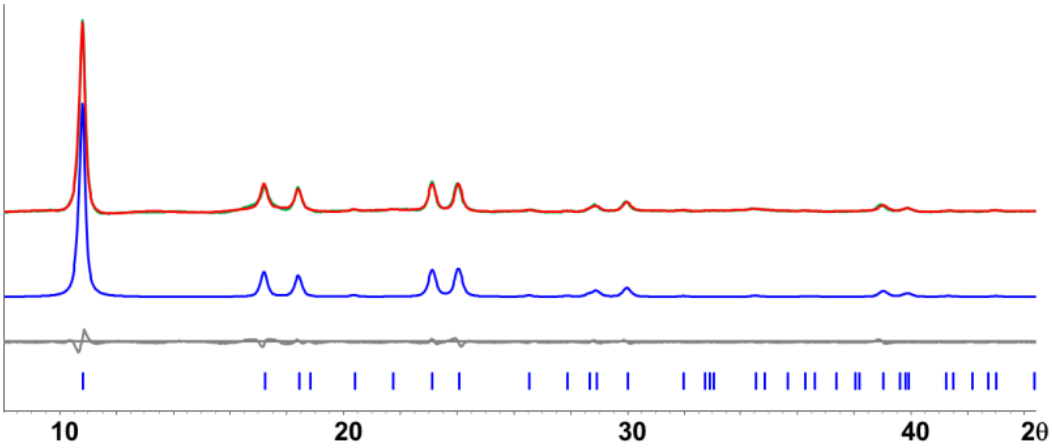

Figure S1. X-ray powder pattern of $LiCo(acac)_3$ (**1**) and the Le Bail fit. Red and green curves are experimental and calculated patterns overlaid. Blue pattern is a calculated single peak pattern and grey line is the difference curve. Theoretical peak positions are shown at the bottom as blue lines.

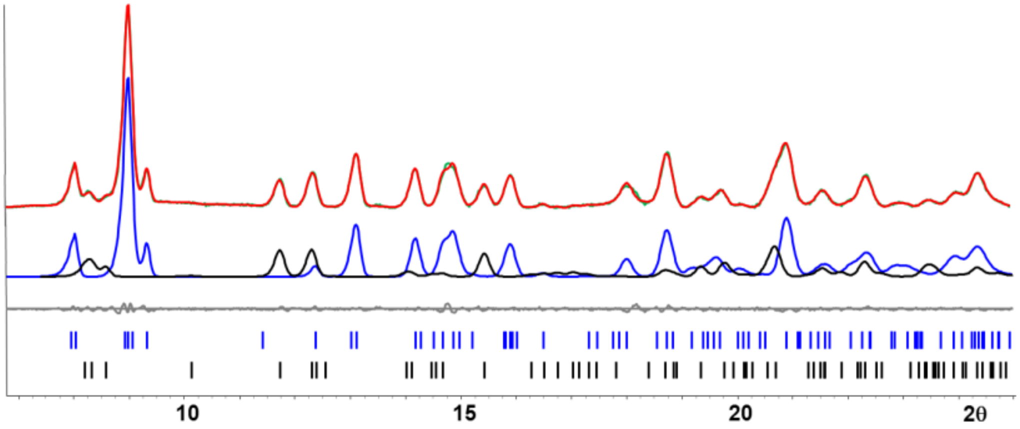

Figure S2. X-ray powder pattern of $LiCo(tbaoac)_3$ (**2**) and the Le Bail fit. Red and green curves are experimental and calculated patterns overlaid. Blue and black patterns are calculated single peak patterns for two polymorph modifications with theoretical peak positions shown at the bottom as blue and black lines (triclinic and monoclinic modifications, respectively). Grey line is the difference curve. Refined unit cell parameters for triclinic and monoclinic modifications are shown in the Table S1. Rietveld refinement against powder pattern of **2** gives the ratio of triclinic (single crystal data for **2**) to monoclinic (modeled using single crystal data for **3**) modifications as 84:16.

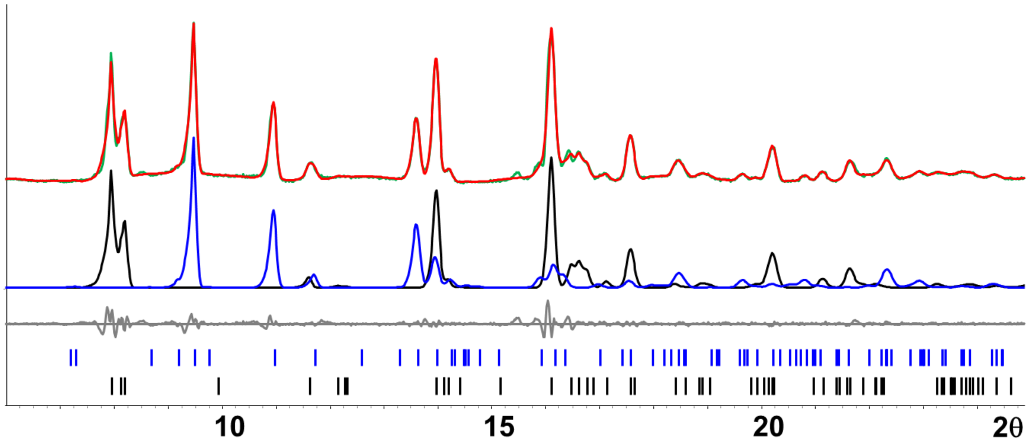

Figure S3. X-ray powder pattern of LiCo(dhd)$_3$ (**3**) and the Le Bail fit. Red and green curves are experimental and calculated patterns overlaid. Blue and black patterns are calculated single peak patterns for two polymorph modifications with theoretical peak positions shown at the bottom as blue and black lines (triclinic and monoclinic modifications, respectively). Grey line is the difference curve. Refined unit cell parameters for triclinic and monoclinic modifications are shown in the Table S1. Rietveld refinement against powder pattern of **3** gives the ratio of monoclinic (single crystal data for **3**) to triclinic (modeled using single crystal data for **2**) modifications as 62:38.

Table S1. Unit cell parameters for triclinic and monoclinic modifications of LiCo(tbaoac)$_3$ (**2**) and LiCo(dhd)$_3$ (**3**) obtained by the Le Bail fit.

	Sp. gr.	*a* (Å)	*b* (Å)	*c* (Å)	*α* (°)	*β* (°)	*γ* (°)
LiCo(tbaoac)$_3$ (**2**)	*P*-1	11.664(1)	12.707(1)	12.958(1)	102.858(8)	111.41(1)	106.562(7)
	*P*2$_1$/*n*	12.389(2)	9.727(2)	21.698(2)		93.00(2)	
LiCo(dhd)$_3$ (**3**)	*P*-1	10.471(4)	12.831(6)	13.444(5)	99.41(2)	110.93(2)	105.38(2)
	*P*2$_1$/*n*	12.132(5)	9.547(4)	21.755(8)		90.60(1)	

Crystal growth

Crystals of LiCo(acac)$_3$ (**1**) suitable for structural measurements were grown by slow diffusion of diethyl ether into the saturated methanol solution of **1** at room temperature. Block-shaped crystals of Co(tbaoac)$_2$, LiCo(tbaoac)$_3$ (**2**), and LiCo(dhd)$_3$ (**3**) were obtained by sublimation in evacuated glass ampule placed in an electric furnace at 140 ^{o}C with a temperature gradient of approximately 5 ^{o}C along the length of container.

Table S2. Crystal growth data for LiCoL$_3$ (L = acac(**1**), tbaoc(**2**), dhd(**3**) and Co(tbaoac)$_2$.

	LiCo(acac)$_3$ (**1**)	Co(tbaoac)$_2$	LiCo(tbaoac)$_3$ (**2**)	LiCo(dhd)$_3$ (**3**)
crystallization temp (^{o}C)	22	140	140	140
color	pink	light-purple	purple	violet
shape	needle	block	block	block

X-ray crystallographic procedures

The single crystal diffraction data for LiCo(acac)$_3$ (**1**), LiCo(tbaoac)$_3$ (**2**), LiCo(dhd)$_3$ (**3**) and Co$_3$(tbaoac)$_6$ were measured on a Bruker SMART APEX CCD-based X-ray diffractometer system equipped with a Mo-target X-ray tube (λ = 0.71073 Å). Data reduction and integration were performed with the Bruker software package SAINT. Data were corrected for absorption effects using the empirical methods as implemented in SADABS. The structures were solved and refined by full-matrix least-squares procedures using the Bruker SHELXTL (version 6.14) software package. All non-hydrogen atoms were refined anisotropically unless noted otherwise. Hydrogen atoms were included in idealized positions for structure factor calculations. Three ^{t}Bu groups were found to be rotationally disordered in **3**. Two out of three disorders were modeled with isotropic parameters using similarity restraints. Some bond distances in the disordered moieties were also restrained. For the refinement of the third disordered ^{t}Bu group with anisotropic carbon atoms, same anisotropic displacement parameters for the minor part were used.

Table S3. Crystal data and structure refinement parameters for LiCo(acac)$_3$ (**1**), Co(tbaoac)$_2$, LiCo(tbaoac)$_3$ (**2**) and LiCo(dhd)$_3$ (**3**).

Compound	**1**	Co(tbaoac)$_2$	**2**	**3**
Empirical formula	$C_{15}H_{21}CoLiO_6$	$C_{48}H_{78}Co_3O_{18}$	$C_{48}H_{78}Co_2Li_2O_{18}$	$C_{48}H_{78}Co_2Li_2O_{12}$
Formula weight	363.19	1119.89	1074.84	978.84
Temperature (K)	100(2)	100(2)	100(2)	100(2)
Wavelength (Å)	0.71073	0.71073	0.71073	0.71073
Crystal system	Hexagonal	Monoclinic	Triclinic	Monoclinic
Space group	*R*-3*c*	$P2_1/n$	*P*-1	$P2_1/n$
a (Å)	16.272(3)	9.7761(11)	11.333(2)	12.815(4)
b (Å)	16.272(3)	16.9962(19)	12.275(2)	9.767(3)
c (Å)	10.968(2)	17.5593(19)	12.460(2)	21.674(7)
α (°)	90.00	90.00	104.286(2)	90.00
β (°)	90.00	100.9190(10)	107.918(2)	90.183(4)
γ (°)	120.00	90.00	110.038(2)	90.00
V(Å^3)	2515.0(9)	2864.8(6)	1424.2(5)	2713.0(14)
Z	6	2	1	2
ρ_{calcd} (g·cm^{-3})	1.439	1.298	1.253	1.198
μ (mm^{-1})	1.048	0.923	0.647	0.665
F(000)	1134	1182	570	1044
Crystal size (mm)	0.24×0.12×0.08	0.15×0.15×0.13	0.32×0.30×0.10	0.12×0.10×0.09
θ range for data collection (°)	3.99 – 27.18	1.68 – 27.92	1.87 – 27.91	1.84 – 25.00
Reflections collected	3781	51810	15022	24211
Independent reflections	581 [R_{int} = 0.0672]	6666 [R_{int} = 0.0351]	6493 [R_{int} = 0.0180]	4768 [R_{int} = 0.1264]
Transmission factors (min/max)	0.7870 / 0.9209	0.8740 / 0.8895	0.8198 / 0.9382	0.9245 / 0.9426
Data/restraints/parameters	581/0/38	6666/0/325	6493/24/328	4768/27/317
quality-of-fit[c]	1.006	1.057	1.063	1.069
$R1$,[a] $wR2$[b] ($I > 2\sigma(I)$)	0.0390, 0.0615	0.0321, 0.0812	0.0492, 0.1439	0.0657, 0.1356
$R1$,[a] $wR2$[b] (all data)	0.0314, 0.0607	0.0383, 0.0840	0.0550, 0.1486	0.1173, 0.1522
Largest diff. peak and hole (ē·Å^{-3})	0.277 and -0.342	0.876 and -0.244	1.506 and -0.724	0.544 and -0.619

[a] $R1 = \Sigma||F_o|-|F_c||/\Sigma|F_o|$. [b] $wR2 = [\Sigma[w(F_o^2-F_c^2)^2]/\Sigma[w(F_o^2)^2]]$

[c] Quality-of-fit = $[\Sigma[w(F_o^2-F_c^2)^2]/(N_{obs}-N_{params})]^{½}$, based on all data.

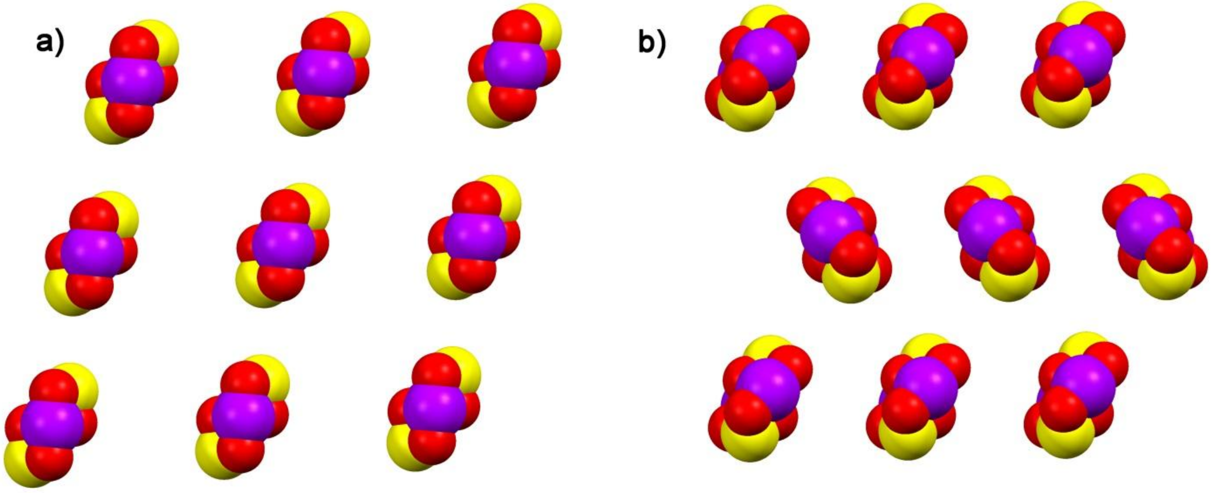

Figure S4. Packing diagrams for a) triclinic modification of LiCo(tbaoac)$_3$ (**2**) and b) monoclinic modification of LiCo(dhd)$_3$ (**3**) rendered as space-filling models. Only [$Li_2Co_2O_6$] cores are shown. Color scheme used: Li-yellow, O-red, Co-purple.

^{1}H and ^{7}Li NMR spectra of heterometallic precursors

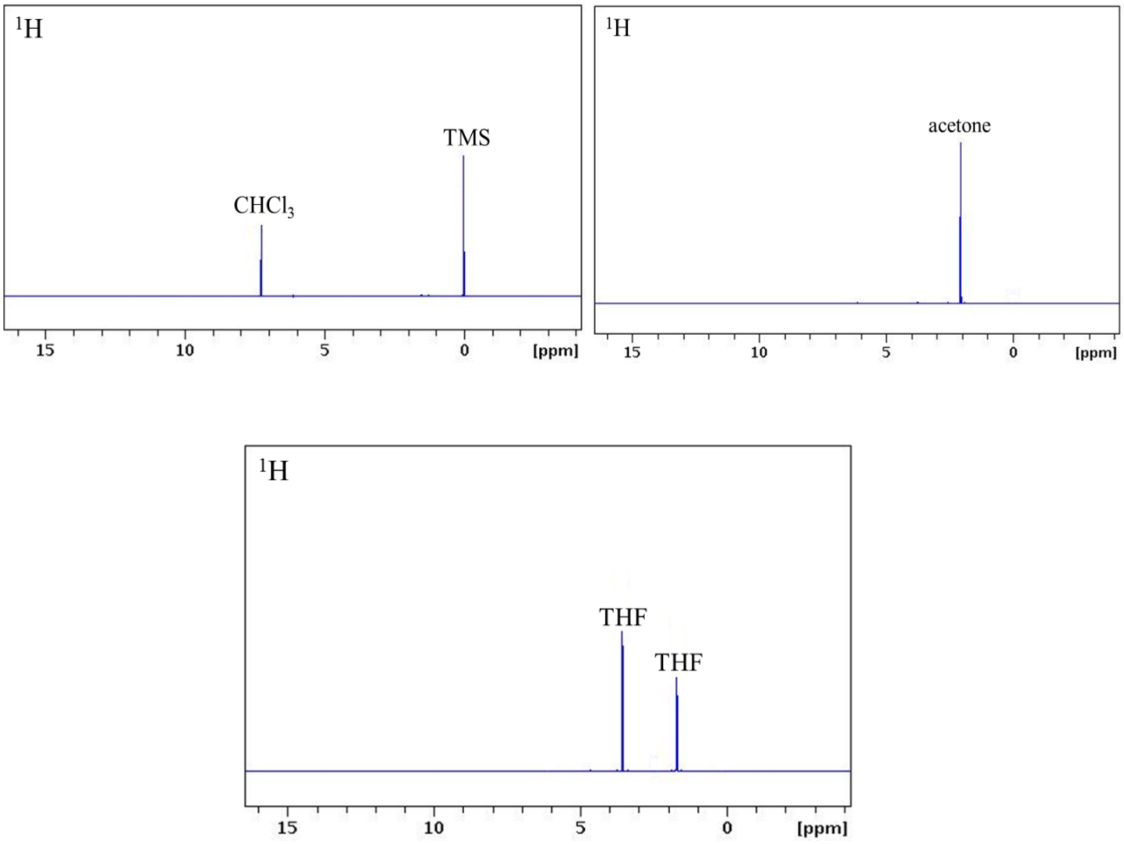

Figure S5. ^{1}H NMR spectra of LiCo(tbaoac)$_3$ (**2**) in CDCl$_3$ (top left), *d*$_6$-acetone (top right) and *d*$_8$-THF (bottom) recorded at room temperature.

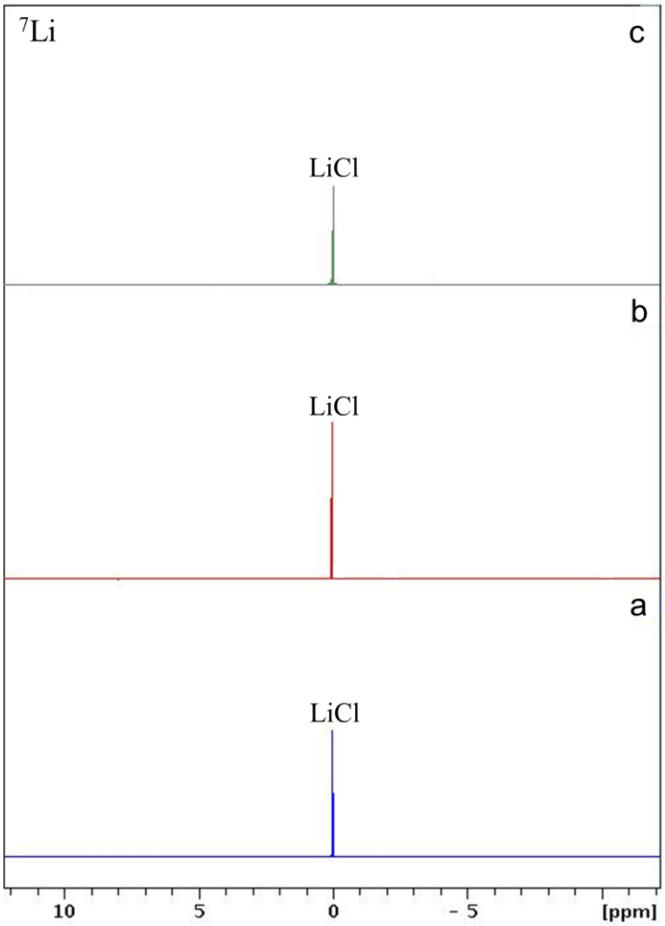

Figure S6. ^{7}Li NMR spectra of LiCo(tbaoac)$_3$ (**2**) in (a) $CHCl_3$, (b) acetone and (c) THF recorded at room temperature.

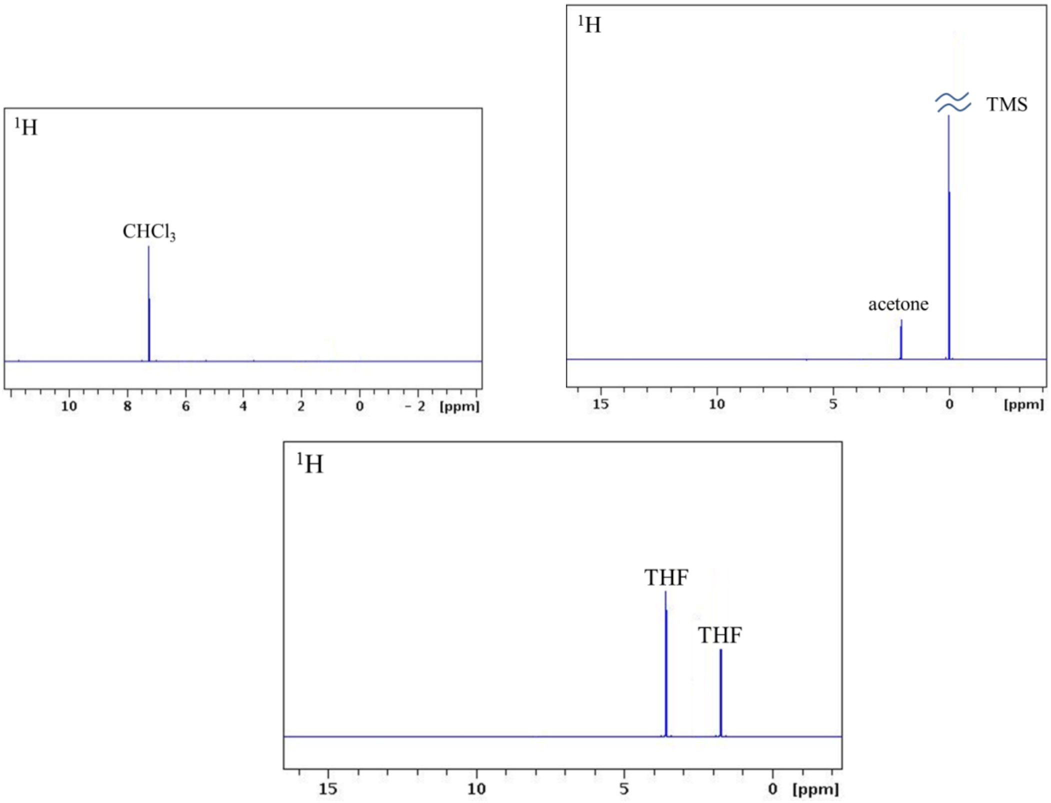

Figure S7. ^{1}H NMR spectra of LiCo(dhd)$_3$ (**3**) in CDCl$_3$ (top left), *d*$_6$-acetone (top right) and *d*$_8$-THF (bottom) recorded at room temperature.

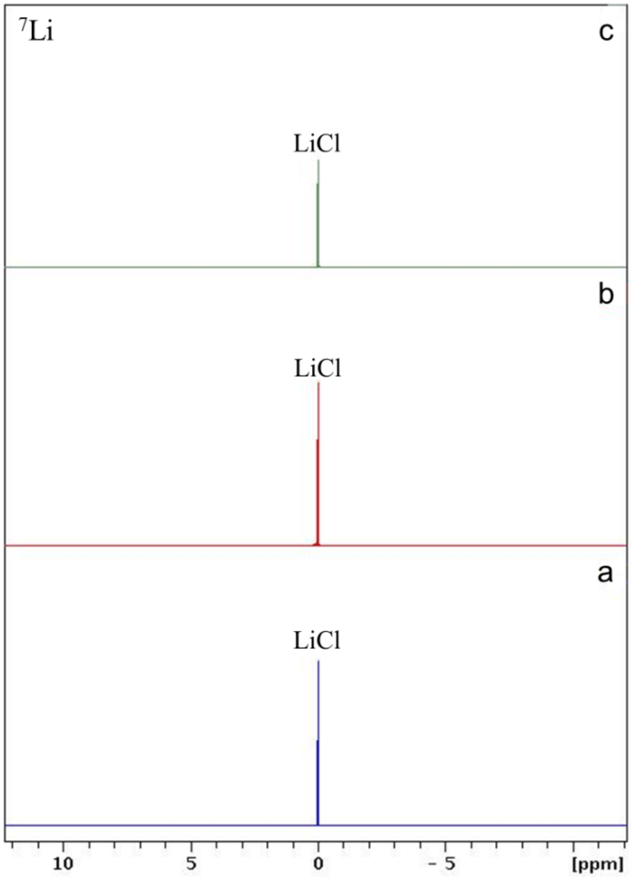

Figure S8. ^{7}Li NMR spectra of LiCo(dhd)$_3$ (**3**) in (a) CHCl$_3$, (b) acetone, (c) THF recorded at room temperature.

ATR-IR spectra of heterometallic precursors

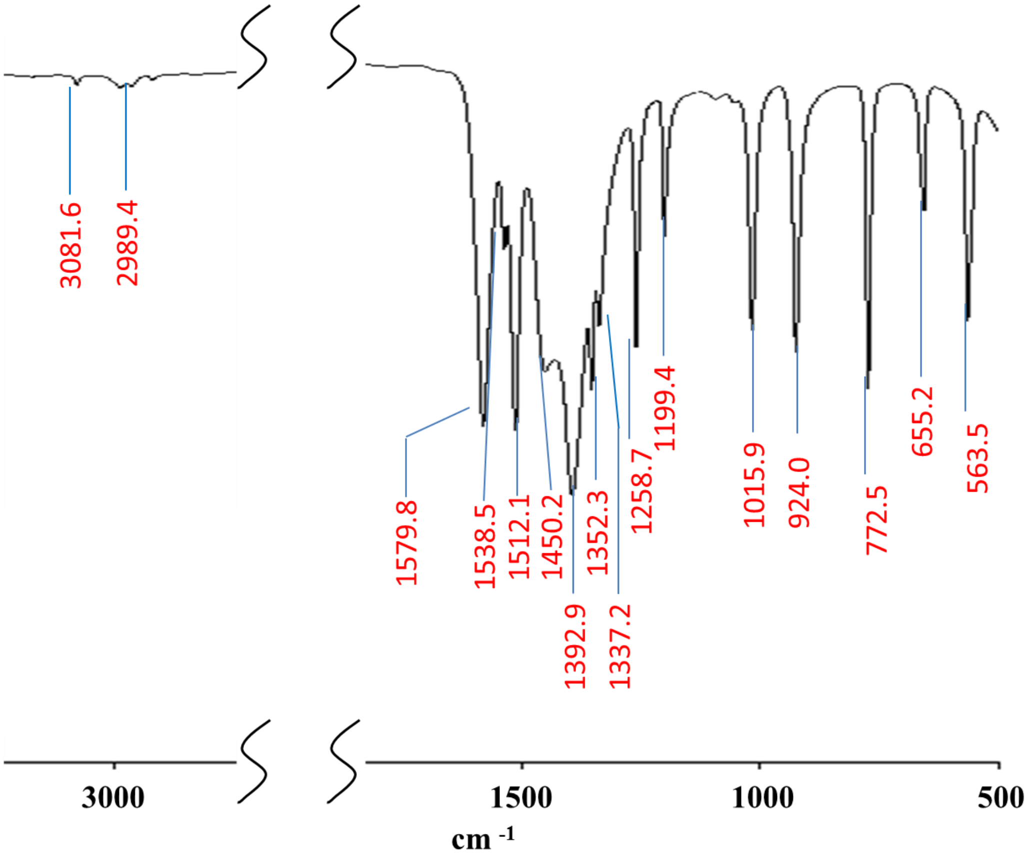

Figure S9. The attenuated total reflection (ATR) spectrum of LiCo(acac)$_3$ (**1**).

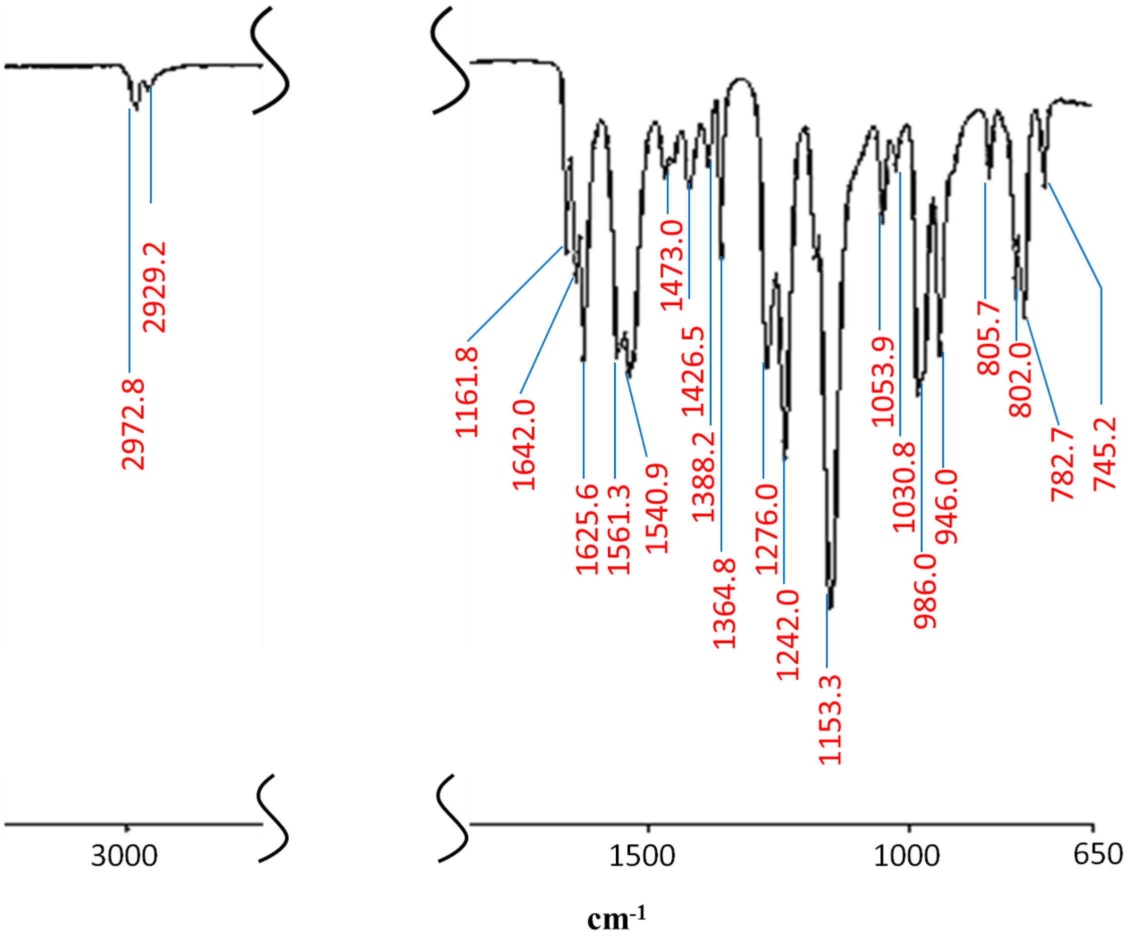

Figure S10. The attenuated total reflection (ATR) spectrum of LiCo(tbaoc)$_3$ (**2**).

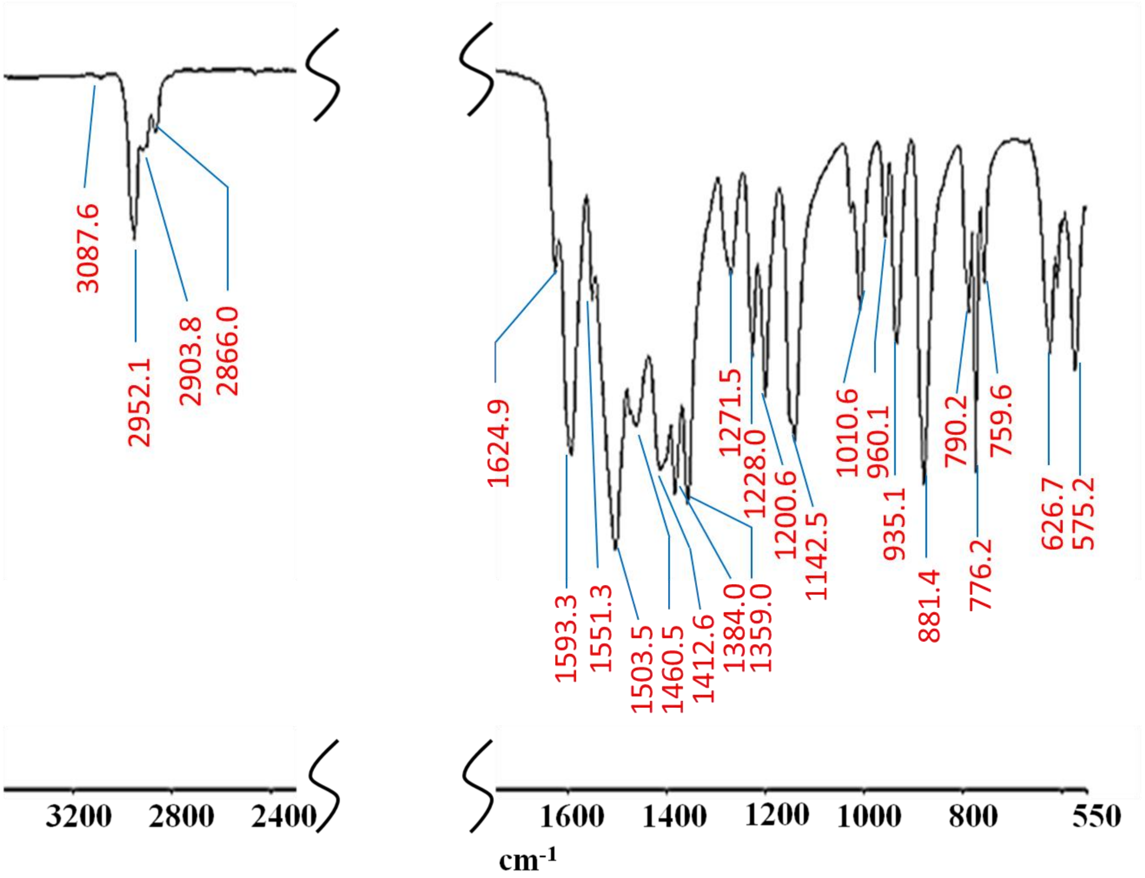

Figure S11. The attenuated total reflection (ATR) spectrum of LiCo(dhd)$_3$ (**3**).

Analysis of decomposition residues of heterometallic precursors

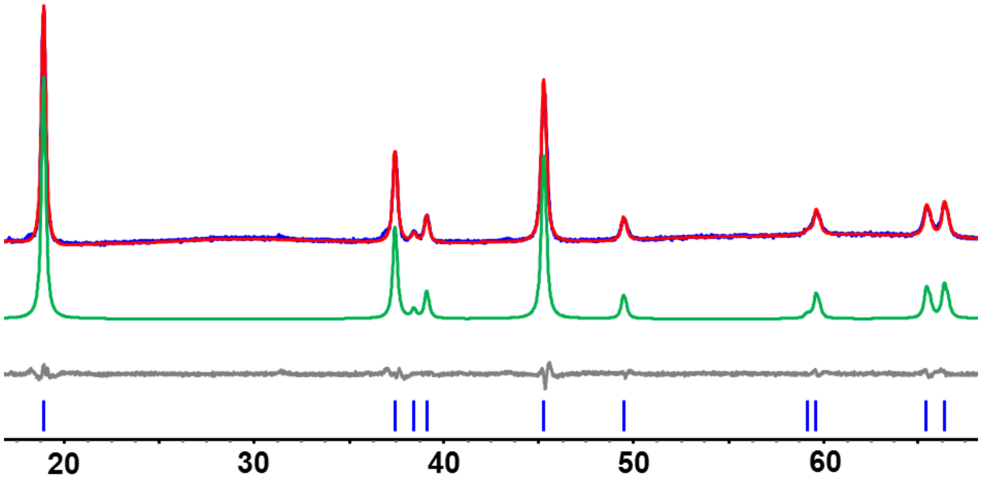

Figure S12. X-ray powder pattern of $LiCoO_2$ obtained by decomposition of complex $LiCo(acac)_3$ (**1**) under oxygen atmosphere at 600 ^{o}C and the Le Bail fit for the trigonal unit cell (Sp. gr. *R-3m*). Blue and red curves are experimental and calculated patterns overlaid. Green curve is a calculated pattern. Grey line is the difference curve. Theoretical peak positions are shown at the bottom.

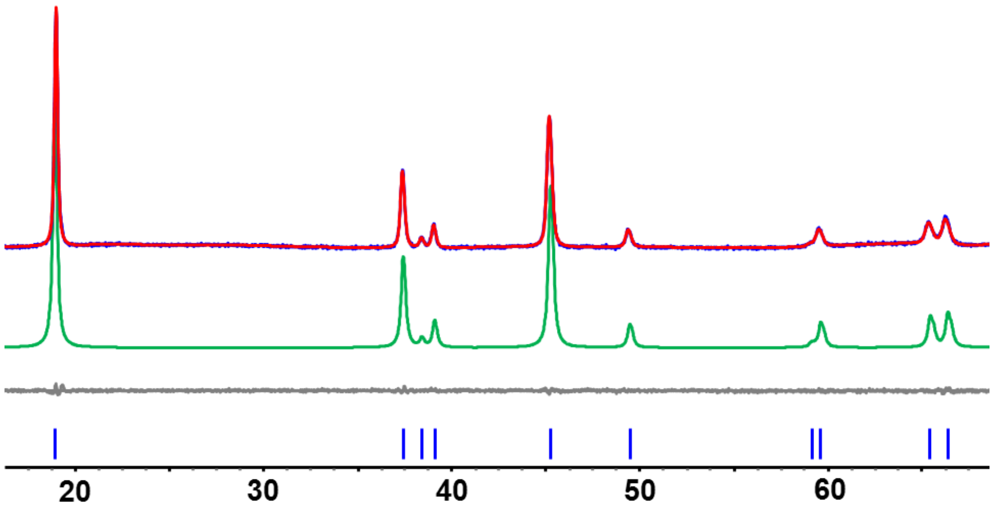

Figure S13. X-ray powder pattern of $LiCoO_2$ obtained by decomposition of complex $LiCo(tbaoac)_3$ (**2**) under air at 600 °C and the Le Bail fit for the trigonal unit cell (Sp. gr. *R-3m*). Blue and red curves are experimental and calculated patterns overlaid. Green curve is a calculated pattern. Grey line is the difference curve. Theoretical peak positions are shown at the bottom.

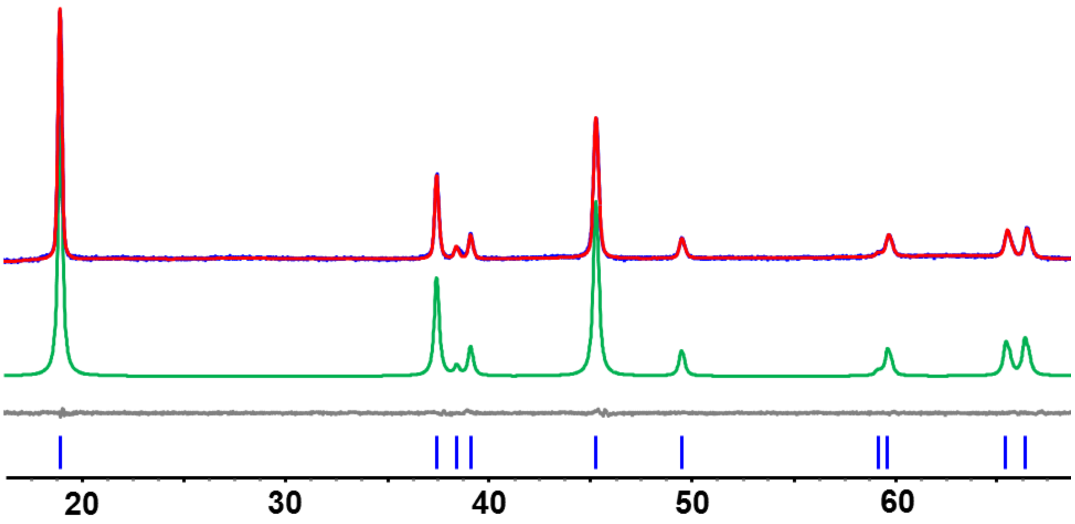

Figure S14. X-ray powder pattern of $LiCoO_2$ obtained by decomposition of complex $LiCo(dhd)_3$ (**3**) under oxygen atmosphere at 700 ^{o}C and the Le Bail fit for the trigonal unit cell (Sp. gr. *R*-3*m*). Blue and red curves are experimental and calculated patterns overlaid. Green curve is a calculated pattern. Grey line is the difference curve. Theoretical peak positions are shown at the bottom.

Table S4. Comparison of the unit cell parameters for $LiCoO_2$ oxide obtained by decomposition of $LiCoL_3$ (L = acac(**1**), tbaoac(**2**) and dhd(**3**)) precursors with the literature data.

	$LiCo(acac)_3$ (**1**)	$LiCo(tbaoac)_3$ (**2**)	$LiCo(dhd)_3$ (**3**)	Literature data[2]
Sp. Gr.	*R*-3*m*	*R*-3*m*	*R*-3*m*	*R*-3*m*
a (Å)	2.8139(1)	2.8154(7)	2.8154(4)	2.8161(5)
c (Å)	14.0494(6)	14.048(4)	14.063(2)	14.0536(5)
V (Å^3)	96.340(6)	96.43(5)	96.54(3)	96.52(3)

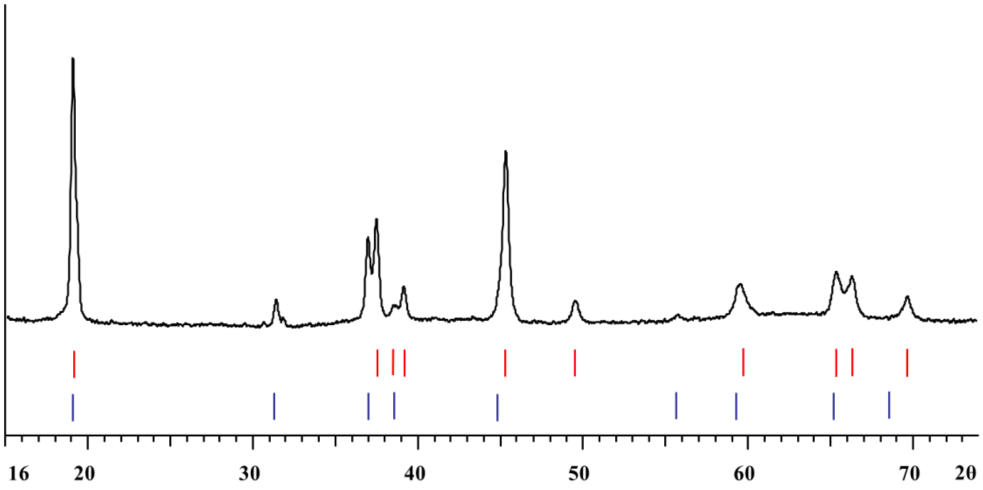

Figure S15. Phase analysis of the sample obtained by decomposition of complex LiCo(acac)$_3$ (**1**) under oxygen atmosphere at 500 °C. Red lines correspond to theoretical peak positions of $LiCoO_2$ (PDF No. 01-070-2685) and blue lines correspond to Co_3O_4 (PDF No. 01-073-1701).

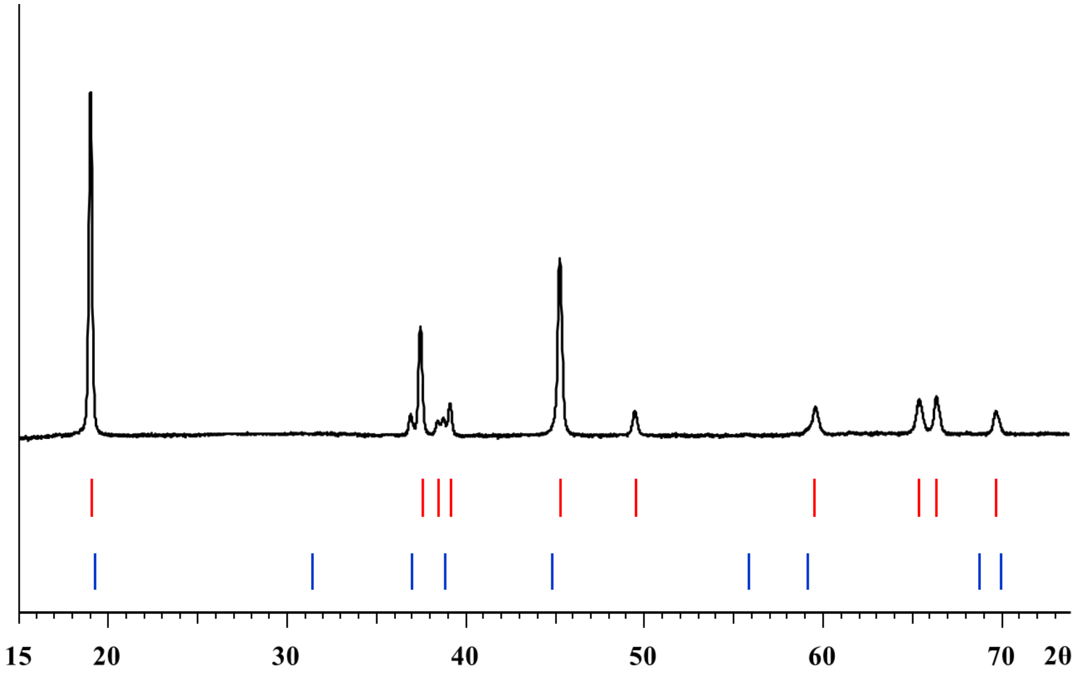

Figure S16. Phase analysis of the sample obtained by decomposition of complex LiCo(dhd)$_3$ (**3**) under oxygen atmosphere at 600 °C. Red lines correspond to theoretical peak positions of $LiCoO_2$ (PDF No. 01-070-2685) and blue lines correspond to Co_3O_4 (PDF No. 01-073-1701).

References

1 P. G. Harris, R. P. Houghton and P. L. Taylor, *Polyhedron*, 1997, **16**, 2651-2658.

2. J. Akimoto, Y. Gotoh and Y. Oosawa, *J. Solid State Chem.*, 1998, **141**, 298-302.